Data-driven Enhancement of SVBRDF Reflectance Data

Heinz Christian Steinhausen, Dennis den Brok, Sebastian Merzbach, Michael Weinmann
and Reinhard Klein

Institute of Computer Science II, University of Bonn, Bonn, Germany

Keywords: Appearance, Spatially Varying Reflectance, Reflectance Modeling, Digitization.

Abstract: Analytical SVBRDF representations are widely used to represent spatially varying material appearance depending on view and light configurations. State-of-the-art industry-grade SVBRDF acquisition devices allow the acquisition within several minutes. For many materials with a surface reflectance behavior exhibiting complex effects of light exchange such as inter-reflections, self-occlusions or local subsurface scattering, SVBRDFs cannot accurately capture material appearance. We therefore propose a method to transform SVBRDF acquisition devices to full BTF acquisition devices. To this end, we use data-driven linear models obtained from a database of BTFs captured with a traditional BTF acquisition device in order to reconstruct high-resolution BTFs from the SVBRDF acquisition devices' sparse measurements. We deal with the high degree of sparsity using Tikhonov regularization. In our evaluation, we validate our approach on several materials and show that BTF-like material appearance can be generated from SVBRDF measurements in the range of several minutes.

1 INTRODUCTION

The accurate digitization of material appearance has been a challenging task for decades. Reproducing fine details of surface reflectance is crucial for a realistic depiction of virtual objects and is of great importance for many applications in entertainment, visual prototyping or product advertisement. Among the widely used reflectance models are analytical spatially varying bidirectional reflectance distribution functions (SVBRDFs) that model the surface reflectance behavior per surface point depending on the view and light configurations. While the acquisition of a sparse set of images taken under different view-light configurations can be achieved within several minutes, the dense information is obtained by means of fitting analytical models to the reflectance samples captured per surface point. For instance, in the recent work by Nielsen et al. (Nielsen et al., 2015), a Tikhonov regularized reconstruction is used to reconstruct isotropic BRDFs from a sparse set of measurements.

However, many materials such as leathers or fabrics show a more complex reflectance behavior including fine effects of light exchange such as inter-reflections, self-occlusions or local subsurface scattering. These effects are not captured by energy-conserving analytical BRDFs. Capturing these ef-

fects requires the use of more complex reflectance representations such as bidirectional texture functions (BTFs) (Dana et al., 1997). These are parameterized on an approximate surface geometry and store spatially varying reflectance behavior depending on the view and light conditions in a data-driven manner within non-energy-conserving apparent BRDFs (aBRDFs) (Wong et al., 1997) per surface point. While a dense sampling of the view and light conditions is required to accurately capture these effects, the acquisition becomes prohibitively costly with time requirements in the order of several hours (Schwartz et al., 2014). To reduce the acquisition effort to only a few hours, den Brok et al. (den Brok et al., 2014) introduced a patch-wise sparse BTF reconstruction based on linear models obtained from a given BTF database.

In this paper, we extend the Tikhonov regularized sparse reconstruction framework for isotropic BRDFs proposed by Nielsen et al. (Nielsen et al., 2015) towards a more general reflectance reconstruction including the aforementioned complex effects of light transport. Similar to the work of den Brok et al. (den Brok et al., 2014), we consider a prior in the form of a given BTF database to derive basis vectors that are used to represent materials in terms of a linear combination of these vectors. However, in contrast to the approach of den Brok et al. (den Brok et al.,

2014) we do not perform a patch-wise reconstruction of aBRDFs, but use the more memory-efficient point-wise reconstruction of aBRDFs in combination with the more robust Tikhonov regularized reconstruction framework. This allows, in contrast to the approach presented by Nielsen et al. (Nielsen et al., 2015), capturing complex effects of light exchange within the reflectance model.

In summary, the key contributions of our work are:

- the practical acquisition of BTFs using SVBRDF acquisition devices and

- a Tikhonov-regularized sparse BTF reconstruction framework based on data-driven linear models.

2 RELATED WORK

While detailed surveys on appearance acquisition and modeling are provided in the literature (Müller et al., 2004; Filip and Haindl, 2009; Haindl and Filip, 2013; Weinmann and Klein, 2015), we focus on the acquisition and modeling of spatially varying reflectance under varying viewing and illumination conditions and only briefly review the corresponding developments.

Reflectance Modeling and Acquisition: In this context, Spatially Varying Bidirectional Reflectance Distribution Functions (SVBRDFs) (Nicodemus et al., 1977) and Bidirectional Texture Functions (BTFs) (Dana et al., 1997) have been widely applied in the literature. While SVBRDFs are parameterized over the surface of a material in terms of storing independent BRDFs at different locations, BTFs represent the reflectance behavior w.r.t. a surface that does not necessarily coincide with the exact surface. This is advantageous when considering materials such as fabrics or leather where the exact surface cannot accurately be reconstructed as their fine structures fall below the resolution of the acquisition device. As BTFs furthermore only rely on apparent BRDFs (Wong et al., 1997) where there is no requirement of energy conservation for the BRDFs stored on the surface, BTFs are capable of capturing mesoscopic effects of light exchange such as inter-reflections, self-occlusions or self-shadowing.

During the acquisition process, images need to be taken from different views and under different illumination conditions which mostly has been realized based on simple camera-light source setups (Lensch et al., 2001), gonioreflectometers (Dana et al., 1997; Matusik et al., 2002; Marschner et al., 2005; Holroyd et al., 2010; Filip et al., 2013), arrays of cameras

and light sources (Furukawa et al., 2002; Weyrich et al., 2006; Schwartz et al., 2011; Ruiters et al., 2012; Nöll et al., 2013; den Brok et al., 2014), combinations of extended light sources and cameras (Aittala et al., 2013) or mobile devices (Aittala et al., 2015).

Sparse Reflectance Acquisition: Instead of relying on a dense sampling of the view-light configurations that can be realized with the respective acquisition setups, several techniques focus on faster and less costly reflectance acquisition from only a suitable subset of these configurations. The non-captured information is interpolated based on certain models.

Such a sparse acquisition has e.g. been followed by Matusik et al. (Matusik et al., 2003a), where a reflectance model based on linear combinations from a set of densely sampled BRDF measurements has been proposed. Similarly, another technique of Matusik et al. (Matusik et al., 2003b) relies on a BRDF database that is used to compute a wavelet basis which allows the representation of isotropic materials from only about 5% of the original data.

Ruiters et al. (Ruiters et al., 2012) presented a compact data-driven BRDF representation where a set of separable functions is fitted to irregular angular measurements. The exploitation of spatial coherence of the reflectance function over the surface makes this technique even capable of reconstructing the appearance of specular materials from sparse measurements. However, the technique is tailored to isotropic materials and cannot be used for too coarse samplings where analytical models are better suited.

Aiming at the compression of BTFs, Koudelka et al. (Koudelka et al., 2003) used linear models computed from apparent BRDFs per material. More recent work by den Brok et al. (den Brok et al., 2014) demonstrated that a sparse BTF acquisition can be obtained for several materials from only about 6% of the view-light configurations taken into account by conventional setups. Alternatively, the sparse acquisition of anisotropic SVBRDFs based on manifold-bootstrapping has been proposed by Dong et al. (Dong et al., 2010). Analytical BRDFs are fitted to the data acquired for certain surface positions and used for the construction of a manifold. Unfortunately, the dimensionality of the manifold of per-texel reflectance functions would be significantly higher for BTFs.

Further work focused on sparse reflectance acquisition based on logarithmic mappings of BRDFs of a database. Nielsen et al. (Nielsen et al., 2015) focus on BRDF reconstruction from an optimized set of view-light-configurations by using a linear BRDF subspace based on a logarithmic mapping of the MERL BRDF

database. This approach has been improved by using priors (Xu et al., 2016) and by its application per point on the material (Yu et al., 2016).

Zhou et al. (Zhou et al., 2016) approach sparse SVBRDF acquisition by modeling reflectance in terms of a convex combination over a set of certain target-specific basis materials and sparse blend priors. Further sparse acquisition approaches include the technique by Vávra and Filip (Vávra and Filip, 2016), that uses a database of isotropic slices, trained from anisotropic BRDFs, to complement sparse measurements of anisotropic BRDFs and the use of a dictionary-based SVBRDF representation (Hui and Sankaranarayanan, 2015). Only involving a mobile device, Aittala at al. (Aittala et al., 2015) perform SVBRDF reconstruction based on pairs of flash and non-flash images. Their approach, however, heavily relies on the stationarity of the texture of the considered materials and the extreme sparse sampling results in non-accurate material depictions. Steinhausen et al. (Steinhausen et al., 2014), as well as Aittala et al. (Aittala et al., 2016), propose the use of guided texture synthesis on sparse reflectance data, the latter relying on deep convolutional neural network statistics.

In this work, we focus on the enhancement of the reflectance representation resulting from a commercially available state-of-the-art SVBRDF acquisition device by replacing the local fitting of analytical BRDF functions by a Tikhonov-regularized sparse reconstruction using data-driven linear models. This allows to consider non-local effects such as inter-reflections, self-occlusions and local subsurface scattering within the reflectance representation and, hence, can be seen as an approach for sparse BTF acquisition.

3 METHOD

Our approach for the digitization of material appearance relies on taking a sparse set of images depicting a material sample under different view/light configurations with a state-of-the-art industry-grade acquisition device, and the subsequent Tikhonov-regularized BTF reconstruction from these sparse measurements using data-driven linear models (see Figure 1). Further details on the individual steps are provided in the following subsections.

3.1 Acquisition Setup

In this work, we used the recently released industry-grade acquisition device *TAC7* (X-Rite, 2016) (see

Figure 1) for the digitization of materials. This device is equipped with four monochromatic cameras mounted on a hemispherical gantry at zenith angles of $5.0°$, $22.5°$, $45.0°$ and $67.5°$ that observe the material sample which is placed on a turntable in the center of the gantry. Furthermore, 30 LED light sources are mounted on the gantry and an additional movable linear light source is included for the acquisition of specular reflectance of the sample. In addition, a projector is integrated in the setup so that the surface geometry can be acquired based on structured light techniques. While four colored LEDs in combination with spectral filter wheels allow the acquisition of spectral reflectance behavior, we do not exploit this feature in the scope of this paper.

The database **D** of densely sampled material BTFs from which the linear models are derived is captured with a traditional BTF acquisition device (Schwartz et al., 2013). This device is equipped with a turntable, which allows a dense azimuthal sampling, and eleven cameras (resolution of $2048 × 2048$ pixels) that are mounted along an arc on an hemispherical gantry with a diameter of about 2m, covering zenith angles between $0°$ and $75°$ with an angular increment of $7.5°$. Furthermore, the gantry is equipped with 198 uniformly distributed light sources.

3.2 Data Acquisition

To gather reflectance samples for each surface point with the TAC7, photos of the considered material sample are taken under different turntable rotations and illuminations for different exposure times. Involved parameters such as the rotation angles of the turntable, the use of the linear light source or the number of exposure steps used for high dynamic range (HDR) imaging can be specified by the user depending on the complexity of the surface geometry and the reflectance behavior of the material to be acquired. For instance, smaller rotation angles of the turntable can be used for complex surface geometry or anisotropic reflectance behavior. Furthermore, the linear light source can be moved in small angular increments to densely sample specular highlights of highly specular materials. After the generation of HDR images for different configurations of turntable and illumination, these are projected onto the surface geometry of the material sample. This allows to gather reflectance samples per surface point for different configurations of view and illumination.

For our experiments, we took images using all four cameras, the 28 monochrome LEDs for luminance and 4 colored LEDs for RGB image data. The sampling is depicted in Figure 2. The turntable was
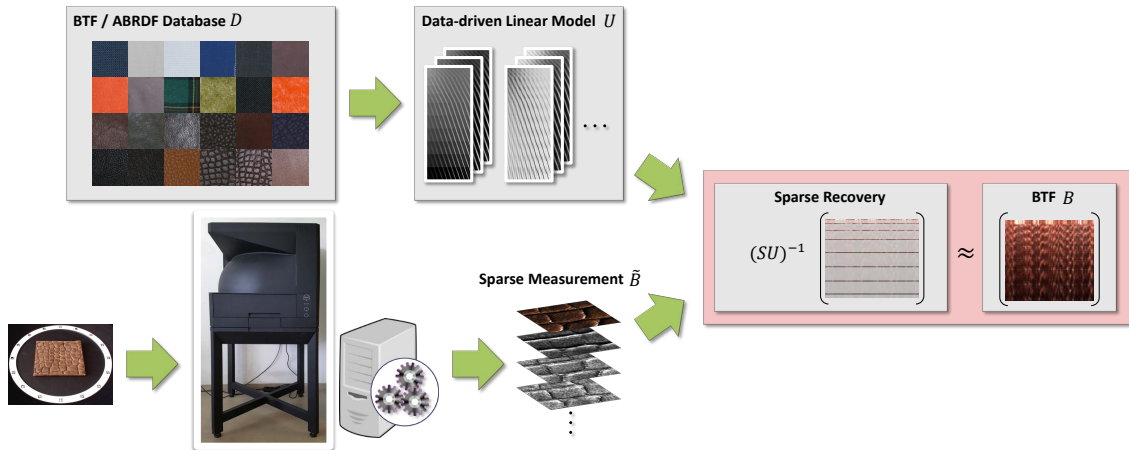
Figure 1: Overview of the proposed pipeline: Reflectance samples for a sparse set of view-light configurations are acquired using the X-Rite TAC7 device (bottom row). They serve as input to the proposed Tikhonov-regularized sparse BTF reconstruction using data-driven linear models.
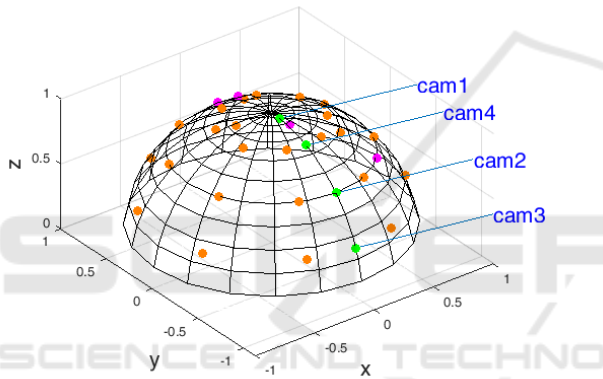

Figure 2: Visualization of the captured view-light configuration. Orange: 24 monochrome LEDs, magenta: 4 LEDs with color filters, green: camera positions.

rotated between $0°$ and $180°$ in steps of $45°$ or $30°$. Measurement times were in the range of $30 - -40$ minutes, while data processing for our chosen patch size of 256×256 texels took up to 90 minutes (without SVBRDF fitting).

3.3 BTF Reconstruction from Sparse Samples

Instead of fitting an analytical Ward BRDF (Ward, 1992) to the sparse reflectance samples per surface point as performed by the TAC7 software (X-Rite, 2016), we fit the sparsely measured data $\tilde{\mathbf{B}}$ to a densely sampled data-driven linear model $\mathbf{U}$, obtained from a database $\mathbf{D}$ of material BTFs.

For the purpose of fitting the sparse TAC7 measurements to the linear model, we represent the set of n_s sparsely measured samples $\tilde{\mathbf{B}}$ in terms of a matrix

product

$$\tilde{\mathbf{B}} = \mathbf{SB}, \tag{1}$$

where $\mathbf{S}$ denotes a binary sparse measurement matrix with $\mathbf{S} \in \{0, 1\}^{n_s \times n_{lv}}$ and $\mathbf{SS}^t = \mathbf{1}$ which selects the TAC7 view-light configurations from the densely sampled measurement $\mathbf{B}$ to be reconstructed, where n_s, n_{lv} denote the number of view-light configurations of the TAC7 device and the DOME II device, respectively. To deal with the fact that the TAC7's camera and light source positions relative to the material sample do not coincide with those in the DOME II device, we perform a simple nearest neighbor search on the normalized positions of lights and cameras, mapping each point in the TAC7's coordinate space to the closest light or camera in the database coordinate space. This is encoded in the measurement matrix $\mathbf{S}$. Note that even for the TAC7 on its own, there are different samplings for color and monochromatic images.

Assuming the existence of a suitable linear model $\mathbf{U}$ that represents $\mathbf{B}$ well, i.e. $\mathbf{B} \approx \mathbf{UV}$ for suitable parameters $\mathbf{V}$, we determine parameters from the sparse measurement $\mathbf{SB}$ via

$$\mathbf{V} = \operatorname{argmin}_{\tilde{\mathbf{V}}} \|\mathbf{SU}\tilde{\mathbf{V}} - \mathbf{SB}\|_F^2 + \|\mathbf{R}\tilde{\mathbf{V}}\|_F^2. \tag{2}$$

The Tikhonov regularization term $\|\mathbf{R}\tilde{\mathbf{V}}\|_F^2$ is included to penalize implausible solutions. Similar to the work on BRDF recovery from a sparse sampling by Nielsen et al. (Nielsen et al., 2015), we use $\mathbf{R} = \lambda \mathbf{1}$, where λ determines the weight of the regularization term. This results in a penalization of large deviations from the distribution of basis coefficients in the training data. However, in contrast to the approach of Nielsen et al. (Nielsen et al., 2015) that is designed for isotropic BRDFs, we focus on the recovery of spatially varying reflectance characteristics in terms of BTFs that include non-local effects of light exchange. Moreover,

Nielsen et al.'s method deals with multi-channel images by considering a single BRDF's color channels as completely different BRDFs in both the training and the testing step. This does not apply to our scenario, where we have to consider monochromatic and color samples from different sample points simultaneously.

In the following, we provide more details on the computation of the employed basis and the BTF reconstruction.

Basis Computation. Given a database $\mathbf{D}$ of BTF measurements such as e.g. the materials introduced by Weinmann et al. (Weinmann et al., 2014), where each BTF is represented by a $n_{lv} \times n_x$ matrix and n_{lv} and n_x denote the number of view-light configurations and the number of texels, respectively, we extract a subset $\mathbf{D_{class}} \subset \mathbf{D}$ for the material class under consideration (e.g. leather, fabric, wool etc.). We concatenate the individual BTFs along the second dimension, i.e. we generate a matrix whose columns contain all of the individual aBRDFs stored within the different BTFs. In order to later be able to consider monochromatic and color samples at once, we first convert the RGB data to YUV color space and compute models for each channel separately; the rationale will become clear in the subsequent section on reconstruction. It is well established that some kind of reduction of dynamic range is necessary in order to avoid obtaining a model mostly concerned with modeling noise in the highlight regions (cf. (Matusik et al., 2003b; Nielsen et al., 2015)). Like den Brok et al. (den Brok et al., 2014), we therefore scale the U and V channels with the corresponding entries from the Y channel, and use the logarithm of the Y channel, such that a pixel tuple (y, u, v) becomes $(\log y, {}^u\!/y, {}^v\!/y)$.

As shown by den Brok et al. (den Brok et al., 2014), a straight-forward approach for BTF basis computation is given by the use of matrix factorization techniques such as the (truncated) singular value decomposition (SVD).

$$\mathbf{D_{class}} \approx \overline{\mathbf{U}} \Sigma \overline{\mathbf{V}}^t. \tag{3}$$

In the following, for brevity we shall write $\mathbf{U}$ for $\overline{\mathbf{U}}\Sigma$. The basis obtained that way is known to generalize well up to some error measure ε for materials $\mathbf{B}$ not contained in the database:

$$||\mathbf{UV} - \mathbf{B}|| < \varepsilon. \tag{4}$$

Contrary to den Brok et al. (den Brok et al., 2014), we use Tikhonov regularization instead of BTF patches for regularization, which makes our method more efficient in terms of computation time and memory consumption. The huge size of the data, however, still makes computing the exact truncated SVD on $\mathbf{D_{class}}$ impossible. Among the many ways to obtain good approximations, we choose to follow den Brok et al. (den Brok et al., 2015) and compute truncated SVDs first for each training material, and subsequently merge the resulting models using eigenspace merging.

Reconstruction. Given a sparse TAC7 measurement $\tilde{\mathbf{B}} = \mathbf{SB}$, we first apply the same color space transformation as above to the RGB part of the data. The monochromatic images are assumed to be pure luminance data (Y-channel of a YUV-triple), and we only apply the logarithm. Because of the color space transformation, we can now deal with each channel separately, and therefore assume our measurement to be of the form $\mathbf{S}_{\log Y}\mathbf{B}_{\log Y}$ and $\mathbf{S}_{\{U,V\}}\mathbf{B}_{\{U,V\}}$. We can then compute approximations $\mathbf{B} \approx \mathbf{UV}$ per channel via

$$\mathbf{V} = ((\mathbf{SU})^t(\mathbf{SU}) + \mathbf{R}^t\mathbf{R})^{-1}(\mathbf{SU})^t(\mathbf{SB}). \tag{5}$$

As mentioned before, the matrix $\mathbf{R} = \lambda\mathbf{1}$ is the Tikhonov regularization term, where λ represents the regularization strength. Note that according to den Brok et al. (den Brok et al., 2015), a typical BTF's U,V channels have a much lower rank than the luminance channel; we can thus hope that the very sparse RGB data from the TAC7 measurement will still suffice for obtaining suitable model parameters.

4 RESULTS

In our experiments, focus on the material class *Leather*, represented by 12 material samples as depicted in Figure 3. For BTF reconstruction, we leave out the material to be reconstructed and compute the linear model on the remaining 11 data sets. For the presented samples, using 512 basis vectors per color channel proved to be sufficient.

Reconstructions of size 256×256 texels were performed on a server equipped with an Intel(R) Xeon(R) E5-2650 CPU, operating at 2.00 GHz, with 128 GB of RAM. Generating a BTF for one material sample took up to ten minutes on this machine, which fits well to the time the TAC7 software takes for computing an SVBRDF for the same sample ($\approx 12 - 15$ minutes) on a desktop computer equipped with an Intel Core i7-4930 processor operating at 3.4 GHz and 32 GB of RAM.

We tried two sampling strategies, involving sample rotations in steps of either $30°$ or $45°$ from $0°$ to $180°$. This yields 480 monochrome and 80 color images in the $45°$-setting and 672 monochrome and
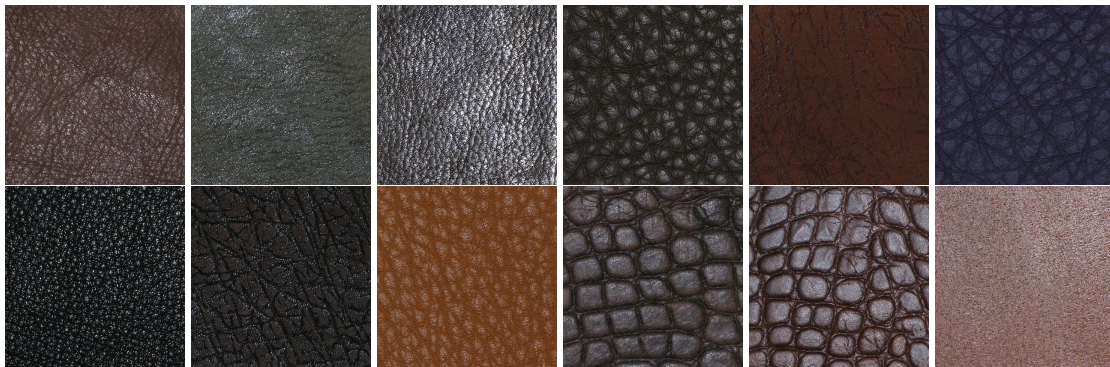
Figure 3: Overview of the samples in the material class *Leather*.

(a) Reference (photo)   (b) $45°; \lambda = (500, 100)$ (c) $45°; \lambda = (5000, 100)$

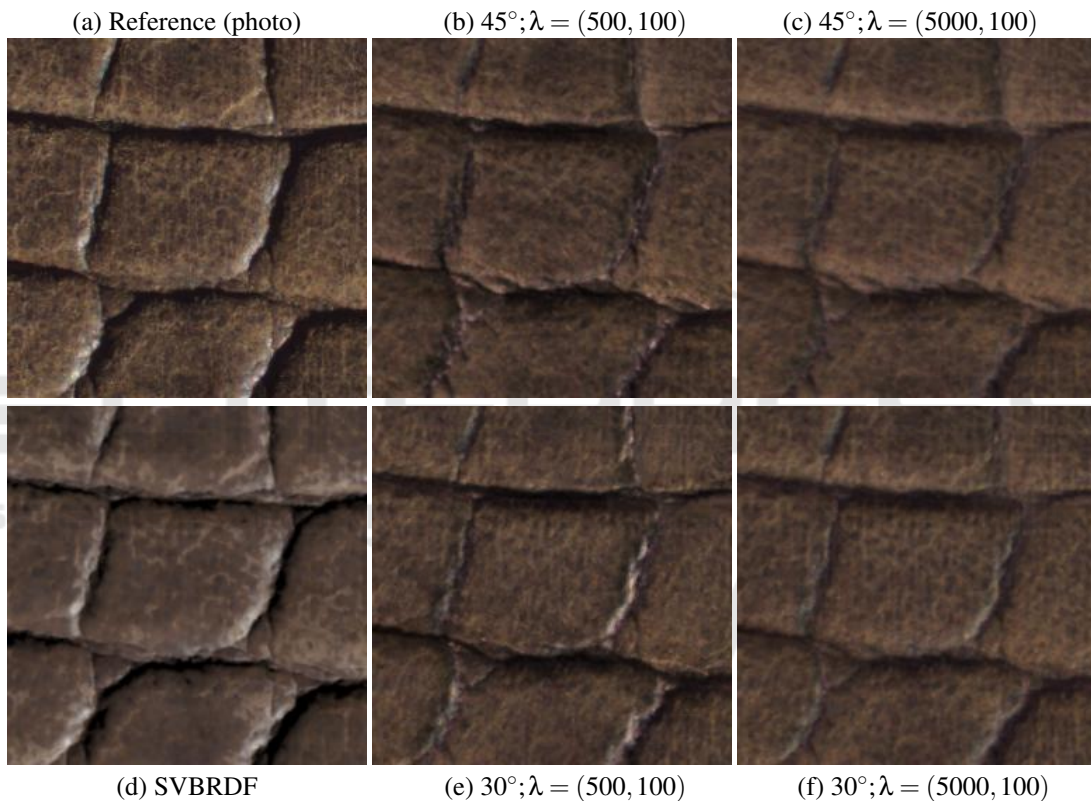(d) SVBRDF   (e) $30°; \lambda = (500, 100)$ (f) $30°; \lambda = (5000, 100)$

Figure 4: Reference image acquired with the TAC7 (a) and corresponding renderings (b-f) of the material sample Leather10, approximating lighting and viewing direction of the real capturing situation. For the rendering shown in (d), we used an SVBRDF computed using the TAC7 software's standard settings, fitting an isotropic Ward model to the measured data, while (b), (c), (e) and (f) illustrate reconstruction results. We used an angular sampling of $45°$ for the BTF reconstruction shown in (b) and (c) and $30°$ for (e) and (f). The middle and rightmost column illustrate the effects of varying weights λ for the Tikhonov regularization term.

112 color images for $30°$. This corresponds to 2.14% respectively 3.00% of the 26 136 images of a typical BTF measurement with the DOME II device (Schwartz et al., 2011). In Figure 4, we provide renderings of the material sample *Leather10* for both sampling strategies in comparison to a rectified, HDR combined input image taken using approximately the same viewpoint and lighting direction, as well as a

rendering from an SVBDRF reconstruction, produced by the software pipeline accompanying the TAC7.

One can observe that the reconstruction result is quite sensitive to the choice of λ weighting the regularization term, especially for the luminance channel. Figure 4 demonstrates this effect by comparing results at $\lambda = (500, 100)$ (luminance, color) and $\lambda = (5000, 100)$. A weight of 5000 for the luminance

component proved to be sufficient, as higher weights did not influence the resulting quality significantly. For the color component, results become stable already at $\lambda \geq 100$.

The visible effect that the highlights in the reconstructions are less pronounced than e.g. in the SVBRDF with its fitted lobe are due to the resampling and compression which took place in preparation of the database.

5 CONCLUSIONS AND OUTLOOK

We have presented a method for turning industrial SVBRDF acquisition devices like the X-rite TAC7 to full BTF capturing devices by means of sparse reconstruction techniques, thereby combining the speed of SVBRDF acquisition with the meso-scale accuracy of BTFs. Compared to the measurement time required when using common devices like the DOME II, ranging around 20 hours, our approach using a ready-to-buy device allows to achieve a usable BTF within under two hours, including image acquisition (≤ 40 minutes), data processing (≤ 90 minutes) and fitting (≈ 10 minutes).

Limitations are especially in the method's ability to model specular highlights which might be missed due to the coarse angular sampling. A logical next step would be to evaluate the applicability of our reconstruction technique to further material classes.

Another use of the TAC7's special capabilities could be BTF spectralization, using the different combinations of LEDs and filters to improve the accuracy in methods for spectral reflectance acquisition such as the method by Dong et al. (Dong et al., 2016).

Another possible enhancement, following Nielsen et al. (Nielsen et al., 2015), as well as den Brok et al. (den Brok et al., 2014) would be to optimize the choice of TAC7 sampling directions depending on the material class.

ACKNOWLEDGEMENTS

REFERENCES

Aittala, M., Aila, T., and Lehtinen, J. (2016). Reflectance modeling by neural texture synthesis. *ACM Trans. Graph.*, 35(4):65:1–65:13.

Aittala, M., Weyrich, T., and Lehtinen, J. (2013). Practical SVBRDF capture in the frequency domain. *ACM Transactions on Graphics (Proc. SIGGRAPH)*, 32(4).

Aittala, M., Weyrich, T., and Lehtinen, J. (2015). Two-shot SVBRDF capture for stationary materials. *ACM Transactions on Graphics (TOG)*, 34(4):110.

Dana, K. J., Nayar, S. K., van Ginneken, B., and Koenderink, J. J. (1997). Reflectance and texture of real-world surfaces. In *1997 Conference on Computer Vision and Pattern Recognition (CVPR '97), June 17-19, 1997, San Juan, Puerto Rico*, pages 151–157. IEEE Computer Society.

den Brok, D., Steinhausen, H. C., Hullin, M. B., and Klein, R. (2014). Patch-based sparse reconstruction of material BTFs. *Journal of WSCG*, 22(2):83–90.

den Brok, D., Weinmann, M., and Klein, R. (2015). Linear models for material BTFs and possible applications. In *Proceedings of the Eurographics Workshop on Material Appearance Modeling: Issues and Acquisition*, pages 15–19. Eurographics Association.

Dong, W., Shen, H.-L., Du, X., Shao, S.-J., and Xin, J. H. (2016). Spectral bidirectional texture function reconstruction by fusing multiple-color and spectral images. *Appl. Opt.*, 55(36):10400–10408.

Dong, Y., Wang, J., Tong, X., Snyder, J., Lan, Y., Ben-Ezra, M., and Guo, B. (2010). Manifold bootstrapping for SVBRDF capture. *ACM Trans. Graph.*, 29(4):98:1–98:10.

Filip, J. and Haindl, M. (2009). Bidirectional texture function modeling: A state of the art survey. *Pattern Analysis and Machine Intelligence, IEEE Transactions on*, 31(11):1921–1940.

Filip, J., Vávra, R., Haindl, M., Žid, P., Krupička, M., and Havran, V. (2013). BRDF slices: Accurate adaptive anisotropic appearance acquisition. pages 1468–1473.

Furukawa, R., Kawasaki, H., Ikeuchi, K., and Sakauchi, M. (2002). Appearance based object modeling using texture database: Acquisition, compression and rendering. pages 257–266.

Haindl, M. and Filip, J. (2013). *Visual Texture: Accurate Material Appearance Measurement, Representation and Modeling*. Springer.

Holroyd, M., Lawrence, J., and Zickler, T. (2010). A coaxial optical scanner for synchronous acquisition of 3D geometry and surface reflectance. *ACM Transactions on Graphics (TOG)*, 29(4):99.

Hui, Z. and Sankaranarayanan, A. C. (2015). A dictionary-based approach for estimating shape and spatially-varying reflectance. In *2015 IEEE International Conference on Computational Photography (ICCP)*, pages 1–9.

Koudelka, M. L., Magda, S., Belhumeur, P. N., and Kriegman, D. J. (2003). Acquisition, compression, and synthesis of bidirectional texture functions. In *ICCV Workshop on Texture Analysis and Synthesis*.

Lensch, H. P. A., Kautz, J., Goesele, M., Heidrich, W., and Seidel, H.-P. (2001). Image-based reconstruction of spatially varying materials. In Gortler, S. J. and Myszkowski, K., editors, *Rendering Techniques 2001: Proceedings of the Eurographics Workshop in*

London, United Kingdom, June 25–27, 2001, pages 103–114, Vienna. Springer Vienna.

Marschner, S. R., Westin, S. H., Arbree, A., and Moon, J. T. (2005). Measuring and modeling the appearance of finished wood. *ACM Transactions on Graphics*, 24(3):727–734.

Matusik, W., Pfister, H., Brand, M., and McMillan, L. (2003a). A data-driven reflectance model. *ACM Trans. Graph.*, 22(3):759–769.

Matusik, W., Pfister, H., Brand, M., and McMillan, L. (2003b). Efficient isotropic BRDF measurement. In *Proceedings of the 14th Eurographics Workshop on Rendering*, EGRW '03, pages 241–247, Aire-la-Ville, Switzerland, Switzerland. Eurographics Association.

Matusik, W., Pfister, H., Ziegler, R., Ngan, A., and McMillan, L. (2002). Acquisition and rendering of transparent and refractive objects. pages 267–278.

Müller, G., Meseth, J., Sattler, M., Sarlette, R., and Klein, R. (2004). Acquisition, synthesis and rendering of Bidirectional Texture Functions. pages 69–94. INRIA and Eurographics Association, Aire-la-Ville, Switzerland.

Nicodemus, F., Richmond, J., Hsia, J., Ginsberg, I., and Limperis, T. (1977). Geometrical considerations and nomenclature for reflectance, natl. *Bur. of Stand. Monogr*, 160.

Nielsen, J. B., Jensen, H. W., and Ramamoorthi, R. (2015). On optimal, minimal BRDF sampling for reflectance acquisition. *ACM Trans. Graph.*, 34(6):186:1–186:11.

Nöll, T., J., K., Reis, G., and Stricker, D. (2013). Faithful, compact and complete digitization of cultural heritage using a full-spherical scanner. pages 15–22.

Ruiters, R., Schwartz, C., and Klein, R. (2012). Data driven surface reflectance from sparse and irregular samples. *Computer Graphics Forum (Proc. of Eurographics)*, 31(2):315–324.

Schwartz, C., Sarlette, R., Weinmann, M., and Klein, R. (2013). DOME II: A parallelized BTF acquisition system. In *Proceedings of the Eurographics Workshop on Material Appearance Modeling*, pages 25–31. The Eurographics Association.

Schwartz, C., Sarlette, R., Weinmann, M., Rump, M., and Klein, R. (2014). Design and implementation of practical bidirectional texture function measurement devices focusing on the developments at the university of Bonn. *Sensors*, 14(5).

Schwartz, C., Weinmann, M., Ruiters, R., and Klein, R. (2011). Integrated high-quality acquisition of geometry and appearance for cultural heritage. pages 25–32.

Steinhausen, H. C., den Brok, D., Hullin, M. B., and Klein, R. (2014). Acquiring bidirectional texture functions for large-scale material samples. *Journal of WSCG*, 22(2):73–82.

Vávra, R. and Filip, J. (2016). Minimal sampling for effective acquisition of anisotropic BRDFs. *Computer Graphics Forum*, 35(7):299–309.

Ward, G. J. (1992). Measuring and modeling anisotropic reflection. *ACM SIGGRAPH Computer Graphics*, 26(2):265–272.

Weinmann, M., Gall, J., and Klein, R. (2014). Material classification based on training data synthesized using a BTF database. In *Computer Vision - ECCV 2014 - 13th European Conference, Zurich, Switzerland, September 6-12, 2014, Proceedings, Part III*, pages 156–171. Springer International Publishing.

Weinmann, M. and Klein, R. (2015). Advances in geometry and reflectance acquisition (course notes). In *SIGGRAPH Asia 2015 Courses*, SA '15, pages 1:1–1:71, New York, NY, USA. ACM.

Weyrich, T., Matusik, W., Pfister, H., Bickel, B., Donner, C., Tu, C., McAndless, J., Lee, J., Ngan, A., Jensen, H. W., and Gross, M. (2006). Analysis of human faces using a measurement-based skin reflectance model. *ACM Transactions on Graphics*, 25:1013–1024.

Wong, T.-T., Heng, P.-A., Or, S.-H., and Ng, W.-Y. (1997). Image-based rendering with controllable illumination. In *Proceedings of the Eurographics Workshop on Rendering Techniques '97*, pages 13–22, London, UK, UK. Springer-Verlag.

X-Rite (2016). Tac7. http://www.xrite.com/categories/Appearance/tac7. accessed at 1st June 2017.

Xu, Z., Nielsen, J. B., Yu, J., Jensen, H. W., and Ramamoorthi, R. (2016). Minimal BRDF sampling for two-shot near-field reflectance acquisition. *ACM Trans. Graph.*, 35(6):188:1–188:12.

Yu, J., Xu, Z., Mannino, M., Jensen, H. W., and Ramamoorthi, R. (2016). Sparse Sampling for Image-Based SVBRDF Acquisition. In Klein, R. and Rushmeier, H., editors, *Workshop on Material Appearance Modeling*. The Eurographics Association.

Zhou, Z., Chen, G., Dong, Y., Wipf, D., Yu, Y., Snyder, J., and Tong, X. (2016). Sparse-as-possible SVBRDF acquisition. *ACM Trans. Graph.*, 35(6):189:1–189:12.